

## Microwave-assisted tunnelling in the presence of dissipation

This article has been downloaded from IOPscience. Please scroll down to see the full text article.

1997 J. Phys. A: Math. Gen. 30 5497

(<http://iopscience.iop.org/0305-4470/30/15/031>)

View [the table of contents for this issue](#), or go to the [journal homepage](#) for more

Download details:

IP Address: 171.66.16.108

The article was downloaded on 02/06/2010 at 05:50

Please note that [terms and conditions apply](#).

# Microwave-assisted tunnelling in the presence of dissipation

G J Papadopoulos<sup>†</sup>

Department of Natural Sciences, University of Cyprus, PO Box 537, CY 1678 Nicosia, Cyprus

Received 22 November 1996, in final form 28 February 1997

**Abstract.** The case of an electron tunnelling through a parabolic repeller and acted upon by a microwave electric field is presently treated taking account of dissipation. Dissipation is introduced using a frictional force and the relevant quantum mechanics stems from an appropriate Lagrangian capable of generating the dissipative force. Considerations are presented for deriving a suitable continuity equation adapted to the dissipative processes involved. Starting with a wavepacket as the particle's initial state, expressions for the probability and current densities, as well as the transmission coefficient, are derived. These are used to see the influence of friction, frequency, amplitude and initial phase of the applied field on the tunnelling effect. Furthermore, the localizing effect of friction is made visible on the reflected portion of the wavepacket, where the main body of the probability resides.

## 1. Introduction

Elberfeld *et al* [1] presented the tunnelling of a wavepacket through an inverted parabolic barrier under the influence of an oscillating field. There the evolution of the tunnelling probability and the current were given in terms of the wavepacket's energy in the absence of the field, as well as the tunnelling probability for various field strengths.

The advent of epitaxial machines has made it feasible to produce in composite semiconductor structures almost tailor-made potentials of minute extent. Thus, it is possible to some degree that a barrier in the form of a parabolic repeller may be made available, but the difficulty with this sort of potential lies in the extensive regions of repulsion, beyond the central peak, which are not involved in the sort of potentials met in tunnelling devices. Nevertheless, the motion of a particle under the combined influence of such a potential together with an alternating driving electric field can be treated exactly, and this was done in [1]. Exactly soluble models are useful as they can provide a good measure of the reliability of numerical treatments and furthermore are expected to supply general insights, which in this case relate to the evolution of the tunnelling phenomenon in the course of time.

In the present work we retain the set-up with the parabolic barrier together with the oscillating field and in addition include dissipation. This is done in some sort of phenomenological way, whereby we begin with a classical Lagrangian able to generate a frictional force in the classical equations of motion, see Havas [2], and then proceed quantizing in the style of Feynman, see Feynman and Hibbs [3]. Historically, the form of a Hamiltonian incorporating a frictional force proportional to the particle's velocity is due to Kanai [4], and goes back as far as 1948. The frictional force provides the means by

<sup>†</sup> Present and permanent address: Department of Physics (Laboratory of Mechanics), University of Athens, Panepistimiopolis, GR 157 84, Zografos, Athens, Greece.

which our particle loses energy to the environment during its motion. Unlike other ways of treating phenomenological dissipation, for example introducing decaying amplitudes, the probability of finding our particle anywhere remains constant at all times. Furthermore, the conjugate operators we employ satisfy the proper commutation relations, and the continuity equation is produced in a way which takes account of the dissipative processes involved. Objections to this sort of approach have been raised by Greenberger [5] and these are dealt with in the next section.

In the literature one finds a considerable amount of work that follows the motion of a wavepacket tunnelling through a barrier in the course of time [6]. Furthermore, tunnelling under the influence of a time-dependent perturbation can be found in [7–11]. Some of the references above involve a double barrier which under certain conditions is known to exhibit high transparency. The transmission coefficient spectrum or, what is related to it, the probability density in momentum representation under the oscillatory action of the modulating field have been found to exhibit side bands, both for single and double barriers [8–11]. In our case we have not been able to detect in the transmission coefficient more than one peak. The same applies to the probability density in momentum representation, but this is not included in the text. This lack is quite likely due to the extensive repulsive range of the potential used, together with its smoothness that enables our particle to acquire a continuous spectrum of energies. A definitive way to explain the absence of side bands relies on the fact that the parabolic repeller does not split the impinging wavepacket into a reflected and a transmitted one<sup>†</sup>. As a result the probability density in momentum space possesses a single peak for a negative momentum at a given time. Further discussion is presented in this respect in section 4. However, our work focuses on the effect of dissipation on the tunnelling phenomenon and this can be treated in an exact fashion in the case of the parabolic repeller.

In section 2 the propagator for our dissipating particle is derived and the evolving wavefunction stemming from an initial wavepacket is obtained. In section 3 the probability and current densities are given explicitly, as well as an expression for the transmission coefficient suitable for considerations involving wavepackets. Finally, in section 4 numerical results follow in which essentially the effect of dissipation, applied field and frequency on tunnelling are shown. Profiles of the reflected portion of the probability density at a given time demonstrate the localization effect of dissipation. In this section we discuss possible sources able to deliver high enough oscillatory electric fields in relation to the strength of the static potential. Suitable sources for the model in question are located in microwave generators.

## 2. Wavepacket evolution

We begin with the classical Lagrangian of our problem

$$L = e^{kt} \left[ \frac{1}{2} m \dot{x}^2 + \frac{1}{2} m \Omega^2 x^2 + eE(t)x \right] \quad (2.1)$$

which when fed into Lagrange's equations of motion supplies the following equation

$$m\ddot{x} = m\Omega^2 x - mk\dot{x} + eE(t). \quad (2.2)$$

Clearly, (2.2) involves the frictional force  $-mk\dot{x}$ , which is used to imitate a mechanism of dissipation, for example transmission of energy into phonons. This sort of simulation has also been employed to represent the process of loss in energy through radiation from

<sup>†</sup> I am grateful to the referee for drawing my attention to this peculiarity.

an oscillating dipole. See for example Sargent III *et al* [12]. Evidently, the form of the frictional force may differ from case to case, but our aim here is to consider this particular form, and present the appropriate quantum mechanics for the tunnelling situation.

At this point we shall digress and discuss an objection raised with regard to a quantum mechanical interpretation that arose when using Lagrangian (2.1) or the associated Hamiltonian (3.3). Greenberger [5] looked at the form of the generalized momentum  $p = m\dot{x}e^{kt}$ , given in (3.2), and concluded that the particle's mass in the Kanai Hamiltonian increases with time as  $me^{kt}$ . The author has inferred this on the basis that the Lagrangian in question takes the form  $T_k - U$ , i.e. kinetic energy minus potential energy, which is not presently the case. As Havas [2] pointed out, Helmholtz suggested that a Lagrangian need not always be in the form  $T_k - U$ . We point out that with this sort of Lagrangian, when no potential forces are present the generalized momentum, is a constant of motion. Thus, the exponential factor  $e^{kt}$  provides the right factor for obtaining the correct expression for the kinetic momentum  $m\dot{x} = e^{-kt}p$ , the constant  $p$  now being the initial kinetic momentum.

With this sort of Hamiltonian, quantization is effected by replacing the generalized momentum by the operator  $-i\hbar\partial/\partial x$ , and the uncertainty principle remains intact. If, however, one forms the commutator of the kinematic momentum and the position operators this becomes  $e^{-kt}\hbar/i$ , which tends to zero after a very long time. This, although unusual, can be justified for friction, simulating the action of an almost macroscopic medium coupled to the particle, makes the motion as time proceeds more and more predictable.

We now proceed to obtain the propagator associated with the Lagrangian (2.1). For this purpose we need only know the classical path starting  $x'$  at  $t = 0$  and reaching  $x$  at time  $t$ . It is given by

$$X_c(\tau) = e^{-k\tau/2} \left\{ x' \cosh(\Omega'\tau) + \frac{\sinh(\Omega'\tau)}{\sinh(\Omega't)} \left[ xe^{-kt/2} - x' \cosh(\Omega't) - \frac{e}{m\Omega'} \int_0^t e^{k\tau'/2} \sinh[\Omega'(t - \tau')] E(\tau') d\tau' \right] + \frac{e}{m\Omega'} \int_0^\tau e^{k\tau'/2} \sinh[\Omega'(\tau - \tau')] E(\tau') d\tau' \right\} \tag{2.3}$$

where

$$\Omega' = [\Omega^2 + (k/2)^2]^{1/2}. \tag{2.3a}$$

Introducing expression (2.3) into the action formula we obtain the action along the classical path as

$$S(xt|x'0) = \frac{mk}{4}(x'^2 - x^2e^{kt}) + \frac{m\Omega'}{2\sinh(\Omega't)} [(x'^2 + x^2e^{kt}) \cosh(\Omega't) - 2x'xe^{kt/2}] + \frac{e}{m\sinh(\Omega't)} \int_0^t e^{k\tau/2} [xe^{kt/2} \sinh(\Omega'\tau) + x' \sinh(\Omega'(t - \tau))] E(\tau) d\tau + \phi(t) \tag{2.4}$$

where  $\phi(t)$  is a function dependent on time and not on spatial coordinates. It is immaterial in the calculation of probability and current densities, but for reasons of completeness we give its expression

$$\phi(t) = -\frac{e^2}{m\Omega' \sinh(\Omega't)} \int_0^t d\tau \int_0^\tau d\tau' \sinh(\Omega'(t - \tau)) \sinh(\Omega'\tau') e^{k(\tau+\tau')/2} E(\tau) E(\tau'). \tag{2.4a}$$

Since our Lagrangian is quadratic we can employ Van Vleck's formula [13] for the semiclassical propagator and obtain the corresponding propagator exactly, as

$$K(xt|x'0) = \left( \frac{m\Omega'}{2\pi i\hbar \sinh(\Omega't)} e^{kt/2} \right)^{1/2} \exp \left[ \frac{i}{\hbar} S(xt|x'0) \right]. \quad (2.5)$$

We previously employed the above procedure for obtaining the propagator of a damped harmonic oscillator in the context of Brownian motion [14], and we could have derived (2.5) replacing the oscillator frequency  $\Omega$  by  $i\Omega$ . We felt, however, that an independent derivation, more suitable to the needs of the present work, would make the paper more readable.

We, now, consider that the state our charged particle has been initially prepared to be in the form of a wavepacket

$$\Phi(x) = (2\pi\sigma^2)^{-1/4} \exp \left[ -\frac{1}{4\sigma^2}(x-x_0)^2 + \frac{i}{\hbar} p_0(x-x_0) \right]. \quad (2.6)$$

Such a state locates the particle, with a probability having a width of  $\sigma$ , at position  $x_0$ , and with an expected momentum  $p_0$ .  $x_0$  will be taken to be negative, i.e. the particle is initially on the left of the barrier's top.  $p_0$  may be taken as being positive, indicating an incoming wave towards the top of the barrier, or negative for a receding wave.

The evolving wavefunction stemming from (2.6) is obtained using the propagator (2.5) as

$$\Psi(x, t) = \int K(xt|x'0)\Phi(x') dx'. \quad (2.7)$$

The integration over  $x'$  in (2.7) is most easily performed via the transformation  $x' - x_0 = \xi$ , and we obtain

$$\Psi(x, t) = \frac{1}{(2\pi\sigma^2)^{1/4}} \left( \frac{e^{kt/2}}{iG} \right)^{1/2} \exp \left[ \frac{i}{\hbar} S(xt|x_00) - \frac{m\Omega' e^{kt}}{2\hbar G \sinh(\Omega't)} (x - X_0(t))^2 + \frac{i}{\hbar} \phi(t) \right] \quad (2.8)$$

where  $G$  is a complex function of time given by

$$G = \frac{\hbar}{2m\Omega'\sigma^2} \sinh(\Omega't) - i \left[ \frac{k}{2\Omega'} \sinh(\Omega't) + \cosh(\Omega't) \right]. \quad (2.8a)$$

Furthermore  $X_0(t)$  in (2.8) is the classical path satisfying the initial conditions  $X_0(0) = x_0$  and  $m\dot{X}(0) = p_0$ , and is given by

$$X_0(t) = e^{-kt/2} \left[ x_0 \cosh(\Omega't) + \left( \frac{p_0}{m\Omega'} + \frac{kx_0}{2\Omega'} \right) \sinh(\Omega't) + \frac{e}{m\Omega'} \int_0^t e^{k\tau/2} \sinh(\Omega'(t-\tau)) E(\tau) d\tau \right]. \quad (2.9)$$

It is worth noting that wavefunction (2.8) is at all times normalized to unity, which means that our approach, while incorporating a flow of energy out of the system, does not violate the principle of probability conservation.

### 3. Probability and current densities

Once the particle's wavefunction is made available the probability density at position  $x$  and time  $t$  is obtained as per usual from  $\Psi^*\Psi$ . Thus, utilizing (2.8) for the wavefunction the required probability density is given by the expression

$$\rho(x, t) = \frac{1}{(2\pi\sigma^2|G|^2e^{-kt})^{1/2}} \exp\left[-\frac{(x - X_0(t))^2}{2\sigma^2|G|^2e^{-kt}}\right]. \quad (3.1)$$

The conservation of probability becomes evident from (3.1). Furthermore, for this linear problem the probability density reduces to a drifted Gaussian, about the particle's classical position, the spread of which is variable and equals  $\sigma|G|e^{-kt/2}$ . Examining this spread one reaches the conclusion that dissipation helps to keep the probability of finding the particle more localized.

The situation with the current density is not as straightforward as with the probability density, and in order to proceed obtaining an expression for this quantity we need the Hamiltonian associated with the Lagrangian (2.1). We begin with the generalized momentum

$$p = \frac{\partial L}{\partial \dot{x}} = m\dot{x}e^{kt}. \quad (3.2)$$

The Hamiltonian then becomes

$$H = p\dot{x} - L = e^{-kt} \frac{p^2}{2m} - e^{kt} \left[ \frac{m}{2} \Omega^2 x^2 + eE(t)x \right]. \quad (3.3)$$

The Hamiltonian operator is constructed from (3.3) by replacing  $p$  by  $-i\hbar\partial/\partial x$ . Thus, Schrödinger's equation takes the form

$$i\hbar \frac{\partial}{\partial t} \Psi = -e^{-kt} \frac{\partial^2}{\partial x^2} \Psi - e^{kt} \left[ \frac{m}{2} \Omega^2 x^2 + eE(t)x \right] \Psi. \quad (3.4)$$

Bopp [15] obtained a current density expression for the damped harmonic oscillator using wavefunctions that had undergone a certain transformation. However, we can proceed more generally and without having to have recourse to particular transformations pertaining to the problem. Once conservation of probability has been established one can apply the usual procedure of balancing the rate of change of the amount of probability enclosed in a small region to the flow of probability through the encapsulating surface. Subsequent use of Schrödinger's equation (3.4) in conjunction with the divergence theorem provides the equation of continuity from which we are led to an expression for the current density in the form

$$J(x, t) = e^{-kt} \frac{\hbar}{m} \text{Im} \left[ \Psi^*(x, t) \frac{\partial}{\partial x} \Psi(x, t) \right]. \quad (3.5)$$

Formula (3.5) for the current density is valid irrespective of the potential forces, once the dissipative force is of the form  $-mk\dot{x}$ . This is so, for in the process of deriving (3.5) the term involving the potential function on the RHS of (3.4) cancels out, but of course it is used in the equation of motion for determining the wavefunction  $\Psi(x, t)$ .

For the particular case at hand we have

$$J(x, t) = \left\{ e^{-kt} \frac{1}{m} \frac{\partial S}{\partial x} + \frac{\Omega'}{|G|^2 \sinh(\Omega't)} \left[ \cosh(\Omega't) + \frac{k}{2\Omega'} \sinh(\Omega't) \right] (X_0 - x) \right\} \times \rho(x, t). \quad (3.6)$$

Expression (3.6) for the current density reduces to the corresponding equation (43) in [1] by removing dissipation, external field, and taking the particle initially still.

The current density is very useful in problems of tunnelling, for its profiles at a given time supply information about the local movements of the wave associated with the particle. Furthermore, the pair of probability and current densities are equivalent to the wavefunction, but the information they provide is more expressive.

For the purpose of diagnosing a tunnelling state of affairs energy is usually taken in comparison with the barrier's height. In dealing, however, with time-dependent forces and moreover with dissipation, one cannot really talk about energy and in this case as a criterion for tunnelling can be used that for which the classical particle starting from position  $x_0$  and with momentum  $p_0$  must never surpass the location of the barrier's top. Caution has to be taken when extremely narrow wavepackets are used to represent the initial particle state. However, even when all forces involved are conservative energy may not be sufficient to provide the tunnelling condition. This is so, imagine a particle at some distance from the position of the barrier's top with an initial momentum that makes it recede from the barrier, and a situation with just opposite momentum. In both cases the energy is the same, but in the first instance we may have zero or definitely smaller tunnelling effects compared with the second case. However, energy is important for incoming particles.

We wish, now, to discuss ways of calculating the transmission coefficient in the context of time-dependent tunnelling. In an open system having one barrier the position of the top of the barrier separates space into two regions, one with high probability of finding the particle, and another with low probability. Naturally, the flow of probability through the separation point takes place from the high to the low side. If tunnelling is the transport mechanism the flow lasts over an extremely short space of time in the form of a pulse. The situation with a closed system, for example a double well, with infinite walls, is completely different, for the tunnelling mechanism transports the maximum excess of probability in one of the wells onto the other and vice versa at a frequency of the order of the ratio of the energy difference in the lowest two states over  $\hbar$ .

In what follows we shall focus our attention on what happens in the low probability side (assumed to be the right-hand side) of an open system when an initial wavepacket state has been prepared on the other side. Since, the flow of probability takes place in the form of a pulse it is evident that the total amount of probability, transmitted, will not depend on the choice of the passage point, provided we wait long enough. This realization is important, for obtaining the transmission coefficient defined in [16] as the ratio of two probabilities  $B/A$ ,  $A$  being the initial probability of finding the particle on the high probability side and  $B$  the net probability that has migrated onto the other side after a long time. It should be noted that the pulse shape may change from one passage point to another. It is significant to note that even with time-dependent forces in open systems the tunnelling pulse duration is finite. Examples of this effect will be seen in computations which follow in the next section. For the behaviour of migration probability in closed systems see [17].

The probability that has migrated through the passage at  $x_1$  up to time  $t$  is given by

$$B(t) = \int_0^t J(x_1, \tau) d\tau = \int_{x_1}^{\infty} [\rho(x, t) - \rho(x, 0)] dx. \quad (3.7)$$

The equality of the last two members in (3.7) results from integrating the continuity equation. It represents the balance between the probability that has been injected from time 0 to  $t$  in the space from  $x_1$  onwards and the excess probability that has been accumulated up to time  $t$ . In accordance with our previous considerations, the transmission coefficient can be obtained from (3.7) as

$$T = \frac{B(\infty)}{\int_{-\infty}^{x_m} \rho(x, 0) dx} \quad (3.8)$$

where  $x_m$  is the coordinate of the barrier top. While the expression for the transmission coefficient (3.2) in [14] and (3.8) provide the same result, the difference being that  $x_1$ , appearing in  $B(\infty)$  in the present work, need not be  $x_m$ , but any convenient point on the barrier's right.

At this moment we specialize in a driving electric field in the form

$$E(t) = E_0 \sin(\omega t + \varphi). \tag{3.9}$$

This sort of electric field results from polarized beams of coherent radiation. In the optical or infrared regime such driving fields derive from appropriate lasers and for lower frequencies from microwave generators. The particular range of frequencies and amplitudes depends greatly on the ability of the external field to cooperate with the static potential. As far as the external frequency is concerned it is effective in a region of  $\Omega$ , which relates to the strength of the static potential. Furthermore, for the amplitude  $E_0$  to be able to exert an influence on the particle's motion it should have a size a few times tenfold the characteristic field dictated by the model. This will become clearer when relevant numbers are considered in the next section. It so happens that the required power of available sources in the high frequency regime is excessively enormous for delivering sizeable fields. Perhaps free electron lasers suit the purpose. However, the necessary conditions with low frequencies are easily fulfilled using more conventional sources, namely microwave generators.

We now give a note concerning the use of (3.8). Generally, in practice  $B(t)$  can be calculated more easily from the integrated current density, than from the integrated difference in the probability densities. The reason being that the probability density diffuses very quickly and the corresponding integral is made out of an extremely small integrand over an immense interval, while the current integral involves more manageable scales.

However, in the case of the inverted parabola, because of the Gaussian form of the probability density (3.1), following [1, 18], we express the far RHS of (3.7) in terms of error functions and we have

$$B(t) = \frac{1}{2} \left[ \operatorname{erf} \left( \frac{|x_0|}{\sqrt{2}\sigma} \right) - \operatorname{erf} \left( \frac{|X_0(t)|}{\sqrt{2}\sigma |G| e^{-kt/2}} \right) \right] \tag{3.10}$$

$$A = \frac{1}{2} \left[ 1 + \operatorname{erf} \left( \frac{|x_0|}{\sqrt{2}\sigma} \right) \right]. \tag{3.11}$$

It should be noted that if the classical particle crosses over the barrier the minus sign between the error functions in (3.10) becomes plus. As  $t \rightarrow \infty$  the argument of the second error function in (3.10) tends to a constant, say  $Z_0/(\sqrt{2}\sigma)$ . This value is practically achieved just after the tunnelling effect is complete, but the limiting value,  $Z_0$ , can be obtained following routine evaluations, and we just cite the result as

$$\begin{aligned} Z_0 = & \left[ \left( \frac{\hbar}{2m\Omega'\sigma^2} \right)^2 + \left( 1 + \frac{k}{2\Omega'} \right)^2 \right] \left\{ \left( 1 + \frac{k}{2\Omega'} \right) x_0 + \frac{p_0}{m\Omega'} + \frac{eE_0}{m[(\omega^2 + \Omega^2) + (k\omega)^2]} \right. \\ & \times \left( \left[ \left( 1 + \frac{k}{2\Omega'} \right) (\omega^2 + \Omega^2) - \frac{k\omega^2}{\Omega'} \right] \sin \varphi \right. \\ & \left. \left. + \left[ \left( 1 + \frac{k}{2\Omega'} \right) k\omega + \frac{\omega}{\Omega'} (\omega^2 + \Omega^2) \right] \cos \varphi \right) \right\}. \end{aligned} \tag{3.12}$$

Thus,  $B(\infty)$  can be calculated from (3.13) as

$$B(\infty) = \frac{1}{2} \left[ \operatorname{erf} \left( \frac{|x_0|}{\sqrt{2}\sigma} \right) - \operatorname{erf} \left( \frac{|Z_0|}{\sqrt{2}\sigma} \right) \right]. \tag{3.13}$$

Furthermore,  $T$  can be obtained from  $T = B(\infty)/A$ , with  $A$  taken from (3.11).



#### 4. Numerical results

In this section we shall see the effect of varying the dissipation, external field amplitude, frequency, and initial phase through the parameters  $k$ ,  $E_0$ ,  $\omega$ , and  $\varphi$  on the probability and current densities, and try to draw certain general conclusions. We shall form a picture of the situation by considering, depending on the case, probability or current densities, as they evolve in time at a given point, or as they extend in space at a given moment. Certainly, the flow of tunnelling probability through a passage point in the form of a pulse of an extremely short duration is general. We have already reached the result that the amount of probability carried by the pulse does not depend on the position of the passage point, although the shapes assumed by the pulses at two different points are not the same. We shall, furthermore, verify the localizing effect scatterers have on the wavefunction. As far as the particle is concerned the relevant parameters are its initial position,  $x_0$ , and momentum,  $p_0$ , as well as the wavepacket's initial spread,  $\sigma$ . In addition to the probability and current densities, the transmission coefficient will be obtained, as this sort of information is generally useful in studies of transport properties. In the cases considered, the classical particle with positive  $p_0$  may execute the following motions. (i) The particle moves towards the top of the barrier and is then reflected and proceeds to  $-\infty$  (pure tunnelling transport); (ii) the particle surpasses the barrier top, oscillates about it and eventually returns to the LHS, and (iii) the particle crosses over the barrier top and proceeds remaining on the RHS (pure crossover transport).

To facilitate the numerical processing we introduce as units for time,  $T_u = \Omega^{-1}$ , energy,  $E_u = \hbar\Omega$ , length,  $L_u = (\hbar/m\Omega)^{1/2}$ , electric field,  $E_{0u} = \hbar\Omega/eL_u$ , and momentum,  $P_u = mL_u\Omega$ .

The above system of units is quite flexible and can supply the implications deriving from the model for a wide range of the parameters involved, once a certain parameter is fixed. As such we select  $\Omega$ , which characterizes the strength of the potential. Enhanced phenomena are expected to occur at frequencies of the external field near  $\Omega$ , and at high electric field amplitudes, several times tenfold the unit of field  $E_{0u}$ . However, the condition of high electric fields puts a severe constraint on the available sources of coherent radiation needed to produce the oscillatory field.

With the above in mind we have checked the suitability of infrared radiation from a continuous wave laser, in view of their high-power output. However, simple calculations based on the formula

$$E_0 = (P/\varepsilon_0 c)^{1/2} \quad (4.1)$$

connecting the electric field amplitude with the output power intensity  $P$  ( $\text{W cm}^{-2}$ ) in conjunction with the corresponding value of  $E_{0u}$  have led us to exclude this case. This on account of the exceedingly high-power required, which even if realized the sample would not have been able to withstand. We have accordingly gone down to lower frequencies, on the order of GHz. Our calculations are based on a value for  $\Omega = 2\pi$  GHz. This corresponds to a wavelength of 30 cm and a unit of length in the device of  $L_u \approx 0.513 \mu\text{m}$ . The power intensity required to generate an electric field amplitude  $E_0 \approx 102E_{0u}$  is  $18 \text{ W cm}^{-2}$ . Values of electric field amplitude of  $100E_{0u}$  are far beyond the region for tunnelling for low applied frequencies, but are suitable for a tunnelling condition to apply for larger values of  $\omega$ , approximately above  $1.6\Omega$ . Thus, with an electric field amplitude, say  $80E_{0u}$ , and starting to scan the frequency region from 0 to  $3\Omega$  tunnelling conditions prevail up to a certain value of  $\omega$  above which value the particle crosses the barrier over until another frequency is reached when again the tunnelling requirement is restored for larger frequencies. For a

certain region of the intermediate frequencies the classical particle goes beyond the barrier top, but returns to the LHS oscillating a few times, depending on the frequency. The microwave generators can be phase locked fairly well and can supply polarized radiation. Adjustment of the initial phase,  $\varphi$ , of the incident radiation can be attained by displacing the sample from the waveguide exit.

For a given high field amplitude,  $E_0$ , it is the combination of the radiation frequency,  $\omega$ , the phase,  $\varphi$ , and the initial phase point  $(x_0, p_0)$ , at which the particle is located by its initial wavepacket state, that determines the particle's classical path. As pointed out earlier, in the case of time-dependent tunnelling the classical path can be used to diagnose prevalence of tunnelling conditions. Certainly, if the particle, coming from left to right, surpasses in its motion the location of the barrier top and continues travelling to the right we are away from a required state of affairs for tunnelling. In contrast, the tunnelling prerequisite is realized whenever the particle approaches or reaches the barrier top and returns moving backwards. For a given high electric field amplitude and a given phase there may be regions of applied frequency for which the condition for tunnelling is fulfilled and regions for which it is not. We shall present diagrams not only relating to the pure tunnelling, but also to the above hybrid situation.

Keeping all but one of the various parameters fixed we are able to surmise the following.

(i) Existence of tunnelling current even when the particle initially recedes from the barrier. To demonstrate this we use the variation of current density pulses with initial momentum, as depicted in figure 1. Tunnelling is essentially produced by the tendency of the wavepacket to spread too fast. While the barrier reduces this effect to a considerable extent, the particle's momentum depending on its direction plays an enhancing or a diminishing role.

(ii) The localizing effect of dissipation. In figure 2 we show two profiles of the probability density at a given time, one for  $k = 0$  and the other with  $k \neq 0$ . As expected, dissipation makes the motion of the reflected packet slower.

(iii) Increase in friction results in a smaller tunnelling current as expected. See figure 3 which compares two current pulses corresponding to two different values of  $k$ , while the

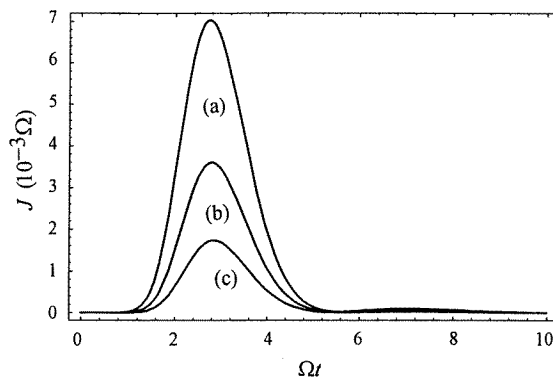


**Figure 1.** This figure shows that tunnelling may exist even for particles initially receding from the barrier. Horizontal axis: time in units of  $\Omega^{-1}$ . Vertical axis: current density in units of  $10^{-3}\Omega$ . The various parameters have been fixed as follows.  $k = 0$ ,  $\varphi = 0$ ,  $\omega = \Omega$ , electric field amplitude  $E_0 = 20\hbar\Omega/eL_u$ , initial particle's position  $x_0 = -30L_u$ , current density taken at  $x_1 = 15L_u$ , initial spread  $\sigma = 8L_u$ , and initial momentum  $p_0$  for curves (a), (b), (c): 2, 0,  $-2mL_u\Omega$  respectively.

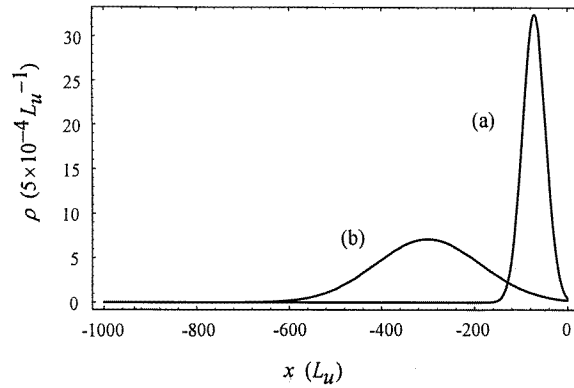


**Figure 2.** Probability density profiles at  $t = 4\Omega^{-1}$  in the high probability side, showing the localizing effect of friction. Horizontal axis: negative  $x$ -axis in units of  $L_u$ . Vertical axis: probability density in units of  $5 \times 10^{-4} L_u$ . Values of parameters as in figure 1, apart from  $k = 3\Omega$  for curve (a) and  $k = 0.5\Omega$  for curve (b), and  $p_0 = -2mL_u\Omega$  for both curves. Clearly, friction causes localization and slows down the motion.

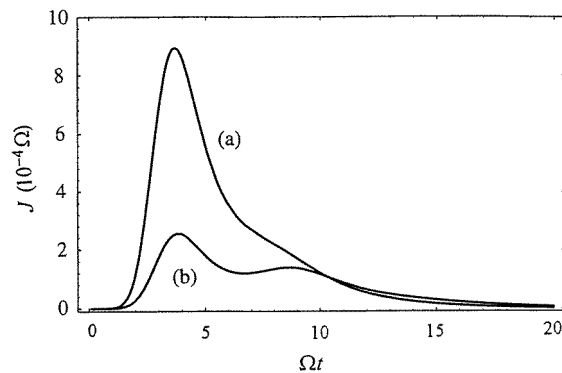


**Figure 3.** This figure shows a drop in tunnelling current when dissipation is increased. Horizontal axis: time in units of  $\Omega^{-1}$ . Vertical axis: current density (at  $x_1 = 15L_u$ ) in units of  $10^{-4}\Omega$ . In (a)  $k = 2\Omega$  and in (b)  $k = 3\Omega$ , while the other parameters remain the same as in figure 2, apart from  $p_0 = 2mL_u\Omega$ .

rest of the parameters are kept fixed.

(iv) A small increase in the initial wavepacket spread results in a substantially higher yield in the tunnelling current. This is demonstrated in figure 4 showing two current pulses having the same parameters apart from the initial spread,  $\sigma$ , taken for two nearby values.

In view of the fact that a narrower initial wavepacket allows higher-energy wavecomponents one may wonder why we are led to a diminished tunnelling current? But, the decomposition of the spatial part of the initial wavepacket provides pairs of waves, one with forward momentum and another with opposite momentum. The wavecomponent with forward momentum enhances the tunnelling effect, while the other with opposite momentum reduces the effect. The net result derives from the combination of all pairs of waves with opposing momenta in conjunction with the mean momentum carrying plane wave. This is depicted in the formulae for the probability and current densities.

We can visualize the enhancing action of increased initial spread by going to the limit

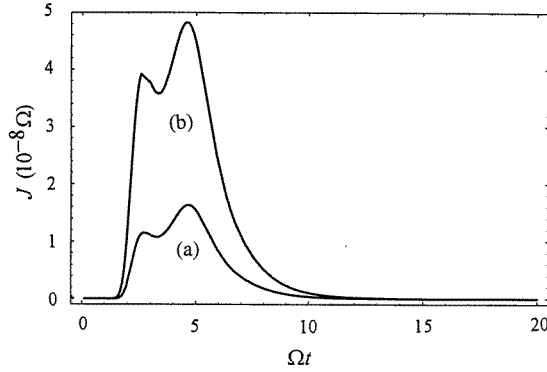


**Figure 4.** This figure shows that a small increase in the initial wavepacket spread results in substantially larger tunnelling current pulse of similar shape. Horizontal axis: time in units of  $\Omega^{-1}$ . Vertical axis: current density (at  $x_1 = 15L_u$ ) in units of  $10^{-8}\Omega$ . The values of the various parameters are now:  $\omega = 2\Omega$ ,  $\varphi = 0$ ,  $k = 0.45\Omega$ ,  $E_0 = 20\hbar\Omega/eL_u$ ,  $x_0 = -40L_u$ ,  $p_0 = 8mL_u\Omega$ , and the initial spread is correspondingly for curves (a), (b)  $\sigma = 5, 5.2L_u$ .

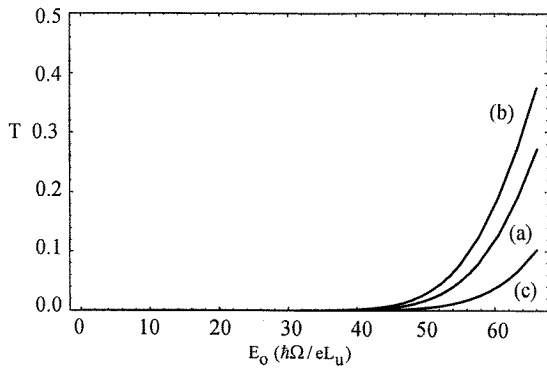


**Figure 5.** Shows that the transmission coefficient increases nonlinearly with increasing electric field amplitude. Horizontal axis: electric field amplitude in units of  $\hbar\Omega/eL_u$ . Vertical axis: transmission coefficient. In all curves the various parameters have values as follows.  $\varphi = 0$ ,  $x_0 = -40L_u$ ,  $p_0 = 8mL_u\Omega$ ,  $\sigma = 5L_u$ ,  $k = 0.8\Omega$ . In curves (a), (b), (c)  $\omega = 0.5, 0.7, 1.2\Omega$  respectively. Examination of the classical paths for the values of the parameters  $\varphi, x_0, p_0, \sigma, k$  as above and all  $\omega$  show that transmission is of a purely tunnelling origin for field amplitude up to  $66\hbar\Omega/eL_u$ .

as  $\sigma \rightarrow 0$ . In this case the probability density (3.1) goes over to

$$\rho(x, t) \rightarrow \delta(x - X_0(t)) \tag{4.2}$$

which is the classical deterministic probability of finding our particle at time  $t$ . Such a classical behaviour excludes tunnelling.

Furthermore, the current density (3.6) in the limit as  $\sigma \rightarrow 0$  takes the form

$$J(x, t) \rightarrow e^{-kt} \frac{1}{m} \frac{\partial S}{\partial x} \delta(x - X_0(t)) \tag{4.3}$$

where the  $\delta$ -function prefactor is the classical velocity acquired by the particle at time  $t$  if it started from  $x_0$  and reached  $x$  in time  $t$ . This, in general, should be noted to differ from  $\dot{X}_0(t)$ . Clearly, on account of (4.3), the current density in the transmission region (beyond

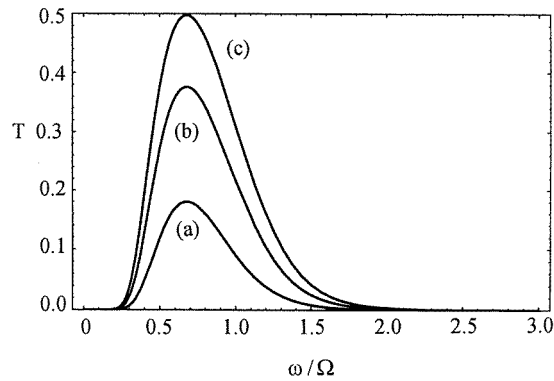


**Figure 6.** Transmission coefficient spectra for different electric field amplitudes. Horizontal axis: frequency in units of  $\Omega$ . Vertical axis: transmission coefficient. In all curves the parameters  $\varphi$ ,  $x_0$ ,  $p_0$ ,  $\sigma$ ,  $k$  are fixed as in figure 5. For curves (a), (b), (c)  $E_0 = 60, 66, 69.1\hbar\Omega/eL_u$  respectively. The value of  $E_0$  in (b) is the largest possible of the associated classical paths irrespective of frequency remain fully within the LHS of the barrier. Thus, spectra (a) and (b) are of a purely tunnelling origin.  $E_0$  in (c) is the maximum value for which for all  $\omega$  the classical particle eventually returns to the LHS. The portion of curve (c) between  $\omega = 0.55\Omega$  and  $\omega = 1.1\Omega$  is associated with classical paths which enter the RHS, but eventually return to the LHS.

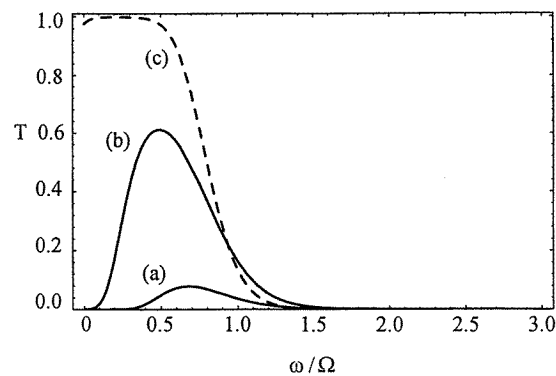


**Figure 7.** This figure shows sensitivity of transmission spectra with initial phase  $\varphi$ . Horizontal axis: frequency. Vertical axis: transmission coefficient. The parameters  $x_0$ ,  $p_0$ ,  $\sigma$ ,  $k$  are fixed as in figure 5 and  $E_0 = 55\hbar\Omega/eL_u$ . In (a)  $\varphi = 0$ , and the spectrum is of completely tunnelling nature. In (b) a difference in  $\varphi$  of  $0.1\pi$  results in a hybrid spectrum consisting of purely tunnelling branches below  $\omega = 0.338\Omega$  and above  $\omega = 0.84\Omega$ , while the in between part of the spectrum relates to paths that enter the RHS. In (c)  $\varphi = 0.3\pi$ . Here over a range of low frequencies full transmission develops, and as the frequency increases the transmission spectrum drops involving crossover processes, followed by barrier overtaking with eventual return to the LHS, and finally for  $\omega \geq 0.95\Omega$  the spectrum becomes of a purely tunnelling origin. In all cases for large enough frequencies the barrier becomes practically opaque.

the barrier top) reduces to zero when the criterion for time-dependent quantum tunnelling prevails.

(v) The tunnelling effect, as expressed through the transmission coefficient for a given initial phase, increases nonlinearly with the electric field amplitude (see figure 5).

(vi) The transmission coefficient spectra, for fixed  $\varphi$ , depend strongly on the applied

field amplitude, as shown in figure 6. As long as the electric field,  $E_0$ , lies below a certain critical value,  $E_{0c}$ , a purely tunnelling spectrum results.  $E_{0c}$  depends on  $x_0$ ,  $p_0$ ,  $\sigma$  and  $k$ . However, for  $E_0 > E_{0c}$  the transmission coefficient spectrum contains a portion around its maximum of non-tunnelling origin (see figure 7). In all cases the spectrum contains only one peak. In contrast to findings in [7–11] no side bands show up. Their absence can be justified on account of the infinite extent of the static potential taken in conjunction with its smoothness. Such a state of affairs allows the particle energy to vary continuously, so that no discernible resonance relating to absorption or emission processes can develop. However, as pointed out in section 1 the absence of side bands can be definitely attributed to the inability of the parabolic barrier to produce a distinct wavepacket in the transmission region. What actually enters the transmission region is just a portion of the RHS tail of the Gaussian wavepacket lying mainly on the reflection side. Prevalence of such a state of affairs excludes from the momentum probability density peaks centred at positive momenta, indicative of side bands in the transmission spectrum.

(vii) The transmission coefficient spectra for a given electric field amplitude vary sensitively with initial phase. See figure 7 which shows a purely tunnelling spectrum, and two spectra of partially tunnelling nature.

### Acknowledgments

This work was performed in the framework of Human Capital Mobility Programme ERBCHRXTCT30124. The author would also like to thank Professor P Razis, Chairman, for the hospitality of his department, in which the work was carried out.

### References

- [1] Elberfeld W, Kleber M, Becker W and Scully M O 1986 *J. Phys. B: At. Mol. Phys.* **19** 2589–97
- [2] Havas P 1957 *Nuovo Cimento Suppl.* **5** 363–88  
Havas P 1973 *Acta Physica Austriaca* **38** 145–67 and references therein  
Helmholtz J 1887 *Reine Angew. Math.* **100** 137
- [3] Feynman R P and Hibbs A R 1965 *Quantum Mechanics and Path Integrals* (New York: McGraw-Hill)
- [4] Kanai E 1948 *Prog. Theor. Phys.* **20** 440–2
- [5] Greenberger D M 1979 *J. Math. Phys.* **20** 761–70  
Greenberger D M 1979 *J. Math. Phys.* **20** 771–80
- [6] Collins S, Lowe D and Barker J R 1987 *J. Phys. C: Solid State Phys.* **20** 6213–32  
Collins S, Lowe D and Barker J R 1987 *J. Phys. C: Solid State Phys.* **20** 6233–43  
Collins S, Lowe D and Barker J R 1988 *J. Appl. Phys.* **63** 142–9
- [7] Azbel M Ya 1992 *Phys. Rev. Lett.* **68** 98–101  
Azbel M Ya 1993 *Phys. Rev. Lett.* **71** 1617–20  
Azbel M Ya 1992 *Phys. Rev. Lett.* **68** 138–41
- [8] Iñarrea J, Platero G and Tejedor C 1994 *Phys. Rev. B* **50** 4581–9  
Iñarrea J, Platero G and Tejedor C 1994 *Semicond. Sci. Technol.* **9** 515–18  
Iñarrea J and Platero G 1995 *Phys. Rev. B* **51** 5244–52
- [9] Jauho A P and Jonson M 1989 *J. Phys.: Condens. Matter* **1** 9027–33  
Jauho A P, Wingreen N S and Meir Y 1994 *Phys. Rev. B* **50** 5228–544
- [10] Wagner M 1994 *Phys. Rev. B* **49** 16544–7  
Wagner M 1995 *Phys. Rev. A* **51** 798–808
- [11] De Raedt H, Garcia N and Huyghebaert J 1990 *Solid State Commun.* **76** 847–50
- [12] Sargent III M, Scully M O and Lamb W E Jr 1974 *Laser Physics* (London: Addison-Wesley) pp 34–5
- [13] Van Vleck J H 1928 *Proc. Natl Acad. Sci., USA* **14** 178–88
- [14] Papadopoulos G J 1973 *J. Phys. A: Math. Gen.* **6** 1479–97
- [15] Bopp F 1962 *Z. Phys.* **14** 699–703
- [16] Papadopoulos G J 1990 *J. Phys. A: Math. Gen.* **23** 935–47

- [17] Papadopoulos G J 1991 *Lecture Notes in Physics* ed V V Dodonov and V I Man'ko (Heidelberg: Springer) pp 475–82
- [18] Dodonov V V and Niconov D E 1991 *J. Sov. Laser Res.* **12** 462–4